Electron paramagnetic resonance study of a new Fe^{3+} centre in $KiTiOPO_4$

Electron paramagnetic resonance study of a new Fe^{3+} centre in $KTiOPO_4$

J F Stenger†, Y Dusausoy†, G Marnier†, H Rager‡ and J M Gaite§

† Laboratoire de Minéralogie et Cristallographie, Unité associée au CNRS 809, Université de Nancy I, BP 239, 54506 Vandoeuvre les Nancy Cédex, France
‡ Institute of Mineralogy, University of Marburg, Hans-Meerwein-Strasse, 3550 Marburg, Federal Republic of Germany
§ Laboratoire de Cristallographie, Unité associée au CNRS 810, Université d'Orléans, rue de Chartres, BP 6759, 45067 Orléans Cédex 2, France

Abstract. An EPR experiment of Fe^{3+} in an iron-doped single crystal of $KTiOPO_4$ was carried out at the Q-band frequency. The angular dependences of the spectra were studied in the three crystallographic planes. The zero-field splitting of Fe^{3+} is of the same order of magnitude as the quantum $h\nu$; so many $\Delta M_S = \pm 2$ transitions were observed together with all the $\Delta M_S = \pm 1$ transitions between spin states. All spin-Hamiltonian parameters were calculated using $\Delta M_S = \pm 1$ or ± 2 transitions for 36 and 18 different orientations, respectively. The use, on the one hand, of the pseudo-symmetries of the fourth-order constants of the spin Hamiltonian and, on the other hand, of structure data and a fourth-order crystal-field calculation for the Ti(2) octahedron allowed us to locate Fe^{3+} in the Ti(2) site. Indeed the octahedron environment of Fe^{3+} does not differ much in orientation from Ti^{4+} and the lattice relaxation is very weak when Fe^{3+} substitutes for Ti^{4+}.

1. Introduction

Potassium titanium phosphate $KTiOPO_4$ (KTP) is currently of considerable interest because it is a most suitable material for frequency doubling of laser radiation (Zumsteg *et al* 1976). KTP crystallises in the orthorhombic space group $Pna2_1$ with eight formula units per unit cell. The structure exhibits two crystallographically different Ti sites: Ti(1) and Ti(2). Both sites are octahedrally coordinated by O and exhibit approximately the same distances and angles within the respective TiO_6 complex (Tordjman *et al* 1974). Zumsteg *et al* have shown that non-linear optical properties of KTP are connected by short bonds: Ti(1)–OT_2 and Ti(2)–OT_1. Also the substitution of Ti atoms by other elements can cause a non-negligible perturbation. However, as far as we know, no studies have been made on impurities in KTP except that of Nizamutdinov *et al* (1987) who reported the incorporation of Fe^{3+} into KTP where Fe^{3+} substitutes for Ti^{4+} in the Ti(1) site. The following questions thus arise. Does Fe^{3+} substitute on both Ti sites? What is the distribution of Fe^{3+} over both sites and how does charge compensation occur? To answer these questions, a further study on Fe^{3+} in KTP is presented.

Table 1. Normalised constants $B_n'^m$ of the spin Hamiltonian in the a, b, c crystallographic axes system in the $Pna2_1$ space group and **g**-tensor components. The errors are as follows: g_{ij}, 10×10^{-4}; $B_2'^m$ and $60B_4'^m$, 15×10^{-5} cm^{-1}.

| Tensor **g**		$B_2'^m$	Value of $B_2'^m$ (10^5 cm^{-1})	$B_4'^m$	Value of $60B_4'^m$ (10^5 cm^{-1})
Component	Value				
g_{XX}	2.0027	$B_2'^0$	1675	$B_4'^0$	217
g_{YY}	2.0026	$B_2'^1$	-6476	$B_4'^1$	71
g_{ZZ}	2.0056	$B_2'^{-1}$	1422	$B_4'^{-1}$	32
g_{XY}	0.0009	$B_2'^2$	-3562	$B_4'^2$	471
g_{XZ}	-0.0011	$B_2'^{-2}$	-1392	$B_4'^{-2}$	172
g_{YZ}	-0.0008			$B_4'^3$	-185
				$B_4'^{-3}$	68
				$B_4'^4$	-120
				$B_4'^{-4}$	-120

2. Experimental procedure

The crystal used for the EPR study has been synthesised by the flux method (Marnier 1986, 1988) and doped with about 300–500 ppm Fe. The grown crystal exhibits two dihedra $\frac{1}{2}\{011\}$ and $\frac{1}{2}\{201\}$, a prism $\{110\}$ and a pinacoid $\{100\}$. This morphology is very helpful for an approximate crystal orientation. The EPR measurements were performed at room temperature using a Varian Q-band spectrometer and 100 kHz modulation. The microwave frequency was calibrated by the resonance magnetic field of DPPH where the magnetic field scale was calibrated using a NMR gaussmeter. To study the accurate angular dependence of the EPR spectra, the crystal was oriented by the X-ray precession method and fixed inside the cavity in such a way that the investigated crystal plane was perpendicular to the rotation axis of the magnet. Small deviations of the crystal setting from the exact orientation could easily be identified by a splitting of the EPR signals. By adjustment of the crystal setting until the splitting vanished, a precise crystal orientation within $\pm 0.2°$ was established for all rotation measurements.

From the angular dependence of the EPR spectra, three allowed transitions ($\Delta M_S = \pm 1$) between spin states were clearly identified: $|-\frac{3}{2}\rangle \leftrightarrow |-\frac{1}{2}\rangle$; $|\pm\frac{1}{2}\rangle$; $|\frac{3}{2}\rangle \leftrightarrow |\frac{1}{2}\rangle$. Then the $B_2'^m$ constants were calculated with $g = 2$ and $B_4'^m = 0$. Once good agreement between experimental and calculated spectra was obtained, the $B_2'^m$ constants were considered to be sufficient to describe the spectra approximately.

To identify the other transition lines belonging to the same spectra (allowed and forbidden transitions), the energy levels were calculated from the $B_2'^m$ values for particular orientations of the magnetic field with respect to the crystal. From those, we were able to identify the allowed transitions between spin states: $|-\frac{5}{2}\rangle \leftrightarrow |-\frac{3}{2}\rangle$; $|\frac{3}{2}\rangle \leftrightarrow |\frac{5}{2}\rangle$. We also found the four forbidden transitions: $|-\frac{5}{2}\rangle \leftrightarrow |-\frac{1}{2}\rangle$; $|-\frac{3}{2}\rangle \leftrightarrow |\frac{1}{2}\rangle$; $|-\frac{1}{2}\rangle \leftrightarrow |\frac{3}{2}\rangle$; $|\frac{1}{2}\rangle \leftrightarrow |\frac{5}{2}\rangle$. Of course, other weaker transitions were present, probably corresponding to the Fe^{3+} centre reported by Nizamutdinov *et al*. Then the 20 parameters of the general spin Hamiltonian (equation (1)) were calculated, using a computer program written by one of us and a coworker (Michoulier and Gaite 1972, Gaite and Michoulier 1973). 36 different orientations in the three crystallographic planes for $\Delta M_S = \pm 1$ and 18 orientations for $\Delta M_S = \pm 2$ were used. The final standard deviation between experimental

Table 2. Characteristics of the second-order term of the spin Hamiltonian expressed in their usual diagonal form.

|	θ (deg)	φ (deg)	
OZ	121.4	-177.3	$B_2'^0 = 0.074\ \text{cm}^{-1}$
OY	-39.9	-40.5	$B_2'^2 = 0.025\ \text{cm}^{-1}$
OX	112.1	78.4	
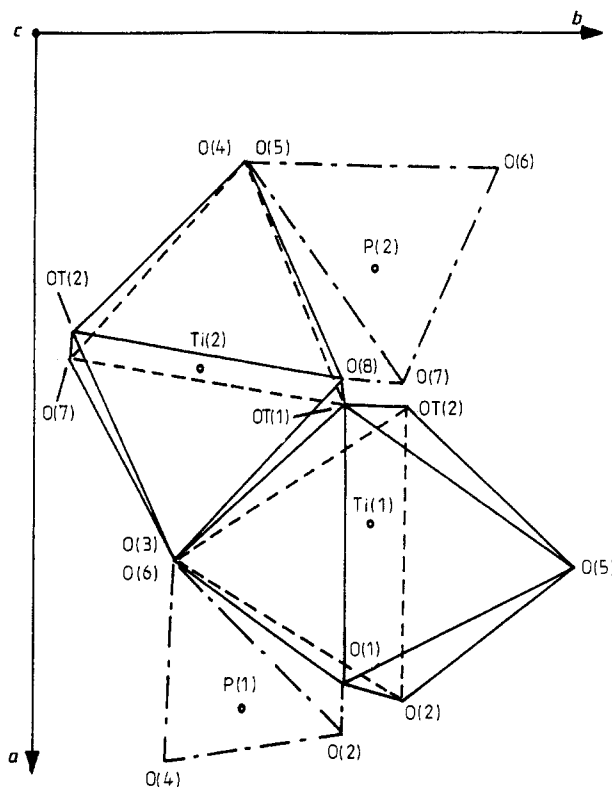
Figure 1. Local crystal structure.

and calculated magnetic fields was 19.5 G. This error is inside experimental accuracy, taking into account that the angular dependence of the spectra varies up to 300 G deg^{-1}.

3. Results and discussion

The EPR spectrum is described by the general Hamiltonian (Abragam and Pryce 1951), for which no particular symmetry of the spin Hamiltonian is expected:

$$\mathcal{H} = \sum_{ij} \beta B_i g_{ij} S_j + \sum_{m=-2}^{2} B_2'^m O_2'^m + \sum_{m=-4}^{4} B_4'^m O_4'^m. \tag{1}$$

g_{ij} ($i, j = X, Y, Z$) are the components of the **g** tensor and $O_n'^m$ the normalised Stevens equivalent operators (Gaite 1987).
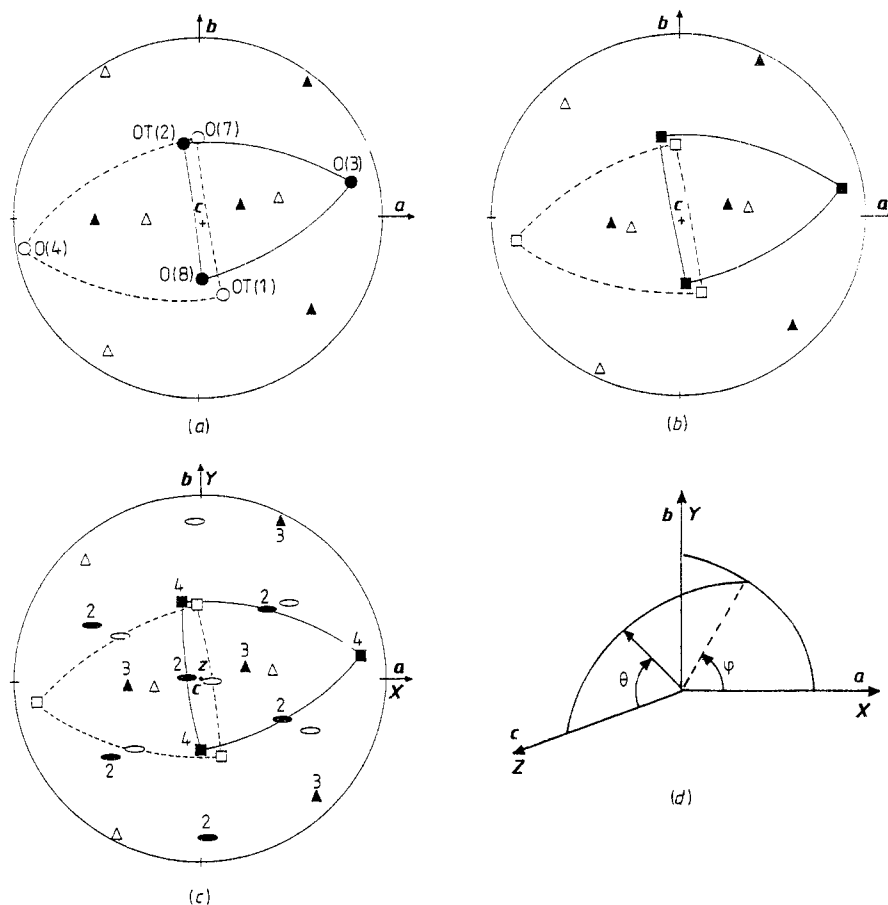
Figure 2. (*a*) Orientations of the Ti–O directions deduced from crystallographic data; (*b*) directions of the 4, 3 pseudo-symmetry axes of the fourth-order crystal field; (*c*) directions of the 4, 3, 2 pseudo-symmetry axes of the $B_4^{\prime m}$ tensor; (*d*) relation between (θ, φ) and the crystallographic axes system.

The values of g_{ij} and of the fine-structure constants $B_n^{\prime m}$ are given in table 1. The **g** tensor is found to be nearly isotropic. The $B_n^{\prime m}$ constants are given in the crystallographic axes system ($X = a$, $Y = b$, $Z = c$). The values of the second-order constants in their and calculated magnetic fields was 19.5 G. This error is inside experimental accuracy, taking into account that the angular dependence of the spectra varies up to 300 G deg^{-1}. Ti(1) octahedron shows that the fine structure constants are of the same order. For example, the energy differences Δ_1 and Δ_2 between the Kramers doublets $|\pm\frac{1}{2}\rangle$, $|\pm\frac{3}{2}\rangle$, $|\pm\frac{5}{2}\rangle$ are 0.8203 cm^{-1} and 0.5973 cm^{-1} for the Ti(1) site and 0.8377 cm^{-1} and 0.5915 cm^{-1} for the Ti(2) site, respectively.

To locate the Fe^{3+} ions in the KTP structure the method developed by Michoulier and Gaite (1972) and by Gaite and Michoulier (1973) was used. It is based on the comparison of the pseudo-symmetry axes of the fourth-order tensor $B_4^{\prime m}$ with the pseudo-symmetry axes of the coordination polyhedron. The fourth-order terms of the spin Hamiltonian are related to the fourth order of the crystal-field development and hence the nearest ligands contribute strongly to these terms.

Table 3. Directions of Ti–O bonds and Ti-face gravity centres in the Ti(2) octahedron, pseudo-symmetries 4 and 3 of fourth-order crystal field, and pseudo-symmetries 4 and 3 of experimental $B_4'^m$ tensor of spin Hamiltonian. The errors are as follows: d, 0.004 Å; θ and φ, 0.5°; ε, 0.006.

	Directions in TiO$_6$ octahedron			Fourth-order crystal field			Experimental $B_4'^m$ tensor		
	Ti(2)–O			Axes 4			Axes 4		
O	d (Å)	θ (deg)	φ (deg)	θ deg	φ (deg)	ε_4	θ (deg)	φ (deg)	ε_4
OT$_1$	1.738	130.7	−73.8	132.1	−75.1	0.0005	137.2	−75.1	0.015
OT$_2$	2.101	45.3	101.3	(47.9	104.9)		(42.8	104.9)	
O$_3$	2.037	81.6	12.5	83.7	9.3	0.0059	83.2	8.6	0.051
O$_4$	1.979	92.8	187.1	(96.3	189.3)		(96.8	188.6)	
O$_7$	1.966	131.6	89.7	137.1	93.6	0.0074	136.6	91.2	0.098
O$_8$	1.994	38.0	−86.2	(42.9	−86.4)		(43.4	−88.8)	

	Ti(2)–gravity centre of the faces			Axes 3			Axes 3		
Face	d (Å)	θ (deg)	φ (deg)	θ (deg)	φ (deg)	ε_3	θ (deg)	φ (deg)	ε_3
O$_3$–OT$_2$–O$_8$	1.398	26.0	16.4	29.2	13.5	0.0084	28.2	12.6	0.097
O$_4$–OT$_1$–O$_7$	0.997	148.0	181.4	(150.8	193.5)		(151.8	192.6)	
O$_4$–O$_8$–OT$_1$	1.048	88.0	51.0	88.5	63.9	0.0088	87.7	63.2	0.102
O$_3$–O$_7$–OT$_2$	1.367	96.3	236.2	(91.5	243.9)		(92.3	243.2)	
O$_3$–OT$_1$–O$_7$	1.078	131.3	15.3	138.5	6.1	0.0087	137.7	6.0	0.103
O$_4$–OT$_2$–O$_8$	1.222	58.0	180.2	(41.5	186.1)		(42.3	186.0)	
O$_3$–O$_8$–OT$_1$	1.081	77.0	320.0	82.0	314.2	0.0088	84.1	313.8	0.100
O$_4$–O$_7$–OT$_2$	1.053	91.4	121.6	(98.0	134.2)		(95.9	133.8)	

Using the following expressions, the direction of the fourfold (ε_4), threefold (ε_3) and twofold (ε_2) pseudo-symmetry axes of the $B_4'^m$ tensor can be calculated from the experimental EPR data:

$$\varepsilon_4(\varphi, \theta) = \sum_{m \neq 0, \pm 4} \frac{B_{4m}'^2(\varphi, \theta)}{S}$$

$$\varepsilon_3(\varphi, \theta) = \sum_{m \neq 0, \pm 3} \frac{B_{4m}'^2(\varphi, \theta)}{S}$$

$$\varepsilon_2(\varphi, \theta) = (B_{41}'^2 + B_{4-1}'^2 + B_{43}'^2 + B_{4-3}'^2)/S$$

with

$$S = B_{40}'^2 + 2 \sum_{m-1}^{4} (B_{4m}'^2 + B_{4-m}'^2)$$

where (θ, φ) is a polar direction with respect to the crystallographic axes system (figure 2d).

Varying these functions with θ and φ, as a minimum is reached, the respective (θ, φ) angles give the direction of a pseudo-symmetry axis. The deviation of the minimum

ε-value from zero indicates the deviation from the true symmetry. Within the ranges $0 \leqslant \varphi < \pi$ and $0 \leqslant \theta < \pi$, we obtained three, four and six minima for ε_4, ε_3 and ε_2, respectively. In order to obtain an impression of the lattice relaxation, a calculation of the fourth-order crystal field was also carried out, using Tesseral harmonics (Hutchings 1964) and the O Cartesian coordinates of the octahedron Ti(2) from crystallographic data (Tordjman *et al* 1974). The pseudo-symmetry axes of this crystal field were calculated in the same way as those of the $B_4'^m$ tensor. The values for (θ, φ) and ε_4, ε_3 are given in table 3.

Figure 2(a) shows a stereographic projection of the Ti–O bond directions and the directions of Ti-face gravity centres in the octahedron, figure 2(b) the directions of the pseudo-symmetry axes 4 and 3 of the fourth-order crystal field calculated for the Ti(2)O_6 octahedron and figure 2(c) the directions of the pseudo-symmetry axes 4 and 3 of the $B_4'^m$ tensor. The agreement between the three stereographic projections is fairly good. Therefore it is concluded that, in the new paramagnetic centre, Fe^{3+} substitutes for Ti(2) in the KTP structure.

Another feature is shown by comparing the Ti–O distances and the experimental ε_4-values. The smallest ε_4-value (0.015) was obtained along the OT_1–Ti(2)–OT_2 direction. This indicates that the deviation from exact fourfold symmetry along this direction is small in agreement with the structural situation around the Ti(2) site. In the perpendicular plane to the OT_1–Ti(2)–OT_2 direction the Ti–O distances are very similar ($\Delta d_{max} = 0.04$ Å) whereas the distances Ti(2)–OT_1 and Ti(2)–OT_2 are quite different ($\Delta d = 0.36$ Å). Furthermore, the same order of the four experimental ε_3-values support the fourfold pseudo-symmetry axis along OT_1–OT_2.

For the undistorted Ti(2)O_6 octahedron, approximately the same ε_4- and ε_3-values were calculated (see table 2). Therefore, it is concluded that the substitution of Ti(2) by Fe^{3+} operates nearly without lattice relaxation and that the actual Fe^{3+} site seems to be the crystallographic Ti(2) site. Further, the charge compensation mechanism must be of long-range order because anionic defects within the nearest or next-nearest coordination sphere or cationic impurities at nearby substitution or interstitial sites are expected to lead to a larger difference between the calculated and experimental ε_4- and ε_3-values.

Nizamutdinov *et al* reported that Fe^{3+} substitutes for Ti^{4+} on the Ti(1) site. The present study shows that Fe^{3+} also substitutes for Ti^{4+} on the Ti(2) site. As both Ti(1) and Ti(2) octahedra exhibit approximately the same distances and angles, Fe^{3+} probably substitutes on the Ti(1) site in the crystal studied.

References

Abragam A and Pryce H M L 1951 *Proc. R. Soc.* A **205** 135–52
Gaite J M 1987 *Electron. Magnetic Resonance of the Solid State* (Soc. Can. Chem.) p 151
Gaite J M and Michoulier J 1973 *J. Chem. Phys.* **59** 488–92
Hutchings M T 1964 *Solid State Phys.* **16** 227–73
Marnier G *Fr. Patent* CNRS 2609976, 29 July 1986 *US Patent* 4746396, 24 May 1988
Michoulier J and Gaite J M 1972 *J. Chem. Phys.* **56** 5205–13
Nizamutdinov N M, Khasanova N M, Bulka G R, Vinokurov V M, Rez I S, Garmash V M and Pavlova N I
    1987 *Sov. Phys.–Crystallogr.* **32** 408–13
Tordjman I, Masse R and Guitel J C 1974 *Z. Kristallogr.* **139** 103–15
Zumsteg F C, Bierlein J D and Gier T E 1976 *J. Appl. Phys.* **47** 4980–5